HHS Public Access

Author manuscript

Cell Immunol. Author manuscript; available in PMC 2020 December 01.

Published in final edited form as:

Cell Immunol. 2019 December ; 346: 103997. doi:10.1016/j.cellimm.2019.103997.

TLR9 signaling mediates adaptive immunity following systemic AAV gene therapy

Scott N. Ashley, **Suryanarayan Somanathan**, **April R. Giles**, **James M. Wilson***

Gene Therapy Program, Department of Medicine, University of Pennsylvania Perelman School of Medicine, Philadelphia, PA 19104, USA

Abstract

An ongoing concern of *in vivo* gene therapy is adaptive immune responses against the protein product of a transgene, particularly for recessive diseases in which antigens are not presented to lymphocytes during central tolerance induction. Here we show that Toll-like receptor 9 (TLR9) signaling activates T cells against an epitope tagged mitochondria-targeted ornithine transcarbamylase (OTC) following the administration of a systemic adeno-associated virus (AAV) vector. Using a transgenic mouse model system, we demonstrate that TLR9 signaling extrinsic to T cells induces a robust cytotoxic *T*-cell response against the transgene and results in transgene expression loss. Overall, our results suggest that inflammation mediated by TLR9 signaling and the presence of high affinity transgene-specific T cells is important for the development of adaptive immune responses to transgene products following AAV gene therapy.

Keywords

AAV; Gene therapy; Adaptive immunity; TLR9; Hepatocyte; $CD8^+$ T cell

1. Introduction

Adeno-associated virus (AAV) vector-mediated gene therapy has shown potential in clinical trials for the treatment of several recessive diseases [1–4]. However, scientists have observed adaptive immune responses to the transgene product in many pre-clinical models [5–8]. These responses are most notable when the delivered gene expresses a “non-self” protein, because the recipient is more likely to develop an immune response to antigens that were not present during lymphocyte development [9–13]. However, adaptive immune responses are

*Corresponding author at: Gene Therapy Program, Department of Medicine, 125 S. 31st Street, TRL 1200, Philadelphia, PA 19104-3403, USA., wilsonjm@upenn.edu (J.M. Wilson).

Author contributions

SNA, SS, and JMW designed and conceived of all experiments. SNA and JMW wrote the manuscript and all authors edited the manuscript. SNA and ARG performed all *in-vivo* experiments. SNA designed and performed fluorescent image analysis.

Competing interests statement

J.M. Wilson is a paid advisor to and holds equity in Scout Bio and Passage Bio; he holds equity in Surmount Bio; he also has a sponsored research agreement with Ultragenyx, Biogen, Janssen, Precision Biosciences, Moderna Therapeutics, Scout Bio, Passage Bio, Amicus Therapeutics, and Surmount Bio which are licensees of Penn technology. JMW is an inventor on patents that have been licensed to various biopharmaceutical companies and for which he may receive payments.

Appendix A. Supplementary data

Supplementary data to this article can be found online at https://doi.org/10.1016/j.cellimm.2019.103997.

tightly controlled, and exposure to a novel protein often results in tolerance rather than immunity if an inflammatory signal is not present [14]. In the case of AAV-mediated gene therapy, the vector genome itself is an immunogenic stimulus that can induce an inflammatory response, which could potentially exacerbate the host's immune response to the transgene.

Toll-like receptor 9 (TLR9), which is located in the endosomal compartment, recognizes unmethylated CpG DNA and induces pro-inflammatory reactions that can result in an immune response [15,16]. Researchers have observed that in response to AAV vectors, TLR9 up-regulates pro-inflammatory cytokines. This observation was reported in studies involving *ex vivo* stimulation of plasmacytoid dendritic cells with AAV2 [17] or i.m. AAV2 administration in mice [18]. Additional studies have shown that immune responses to self-complementary AAV genomes containing double-stranded DNA depend on TLR9 in mice. Specifically, suppressing TLR9 signaling decreased pro-inflammatory cytokine expression and increased systemic levels of the transgene product [19]. Acknowledging that TLR9 plays a role in AAV-induced inflammation, current research has focused on depleting CpG or increasing the CpG methylation state in DNA-based therapies to avoid TLR9-induced inflammatory signaling [20–22]. However, evidence suggests that TLR9 binds the phosphodiester backbone of DNA regardless of the nucleotide sequence, and that CpG motifs merely enhance activation [23]. Therefore, understanding the mechanisms underlying transgene-specific adaptive immune responses is an important step toward the development of safer AAV-mediated gene therapies. In this study, we developed a model system to interrogate transgene-specific immune responses to systemic inflammation caused by TLR9, and investigated the influence of TLR9 on adaptive immune responses following systemic delivery of an AAV vector.

2. Material and methods

2.1. Animals

OT-1 (C57BL/6) and wild-type C57BL/6 mice were acquired from Jackson Laboratory (Bar Harbor, ME). TLR9 −/− (C57BL/6) founders were provided to us by the Koretsky lab (University of Pennsylvania, Philadelphia, PA) and a mouse colony was generated in the Akira lab (Osaka University, Osaka, Japan) [16]. All mice were housed and bred under specific pathogen-free conditions in the Translational Research Laboratory Animal Facility at the University of Pennsylvania.

2.2. Vectors

AAV8 self-complementary h*OTC*co (sc.h*OTC*co), under the control of a TBG promoter containing the G4SVPA poly A signal sequence, was produced by the University of Pennsylvania Vector Core. To generate the sc.h*OTC*co-SIINFEKL transgene cassette, the immunodominant epitope of chicken ovalbumin ($Ova_{257–264}$ SIINFEKL) was cloned into the sc.h*OTC*co transgene immediately following the C-terminal residue. The transgene cassette was produced along with other AAV vectors using an iodixanol step gradient [24].

2.3. Adoptive transfer

Mice received an i.v. injection of 1×10^{11} genome copies of AAV8 expressing either sc.h*OTC*co-SIINFEKL or mutant variants (100 μl total volume diluted in PBS). On day 14 post vector administration, $CD8^+$ T cells were collected from OT-1 mouse spleens using a $CD8^+$ T Cell Isolation kit (Miltenyi Biotec, San Diego, CA). $CD8^+$ *T*-cell purity was > 90%, as measured by flow cytometry. Mice were given 1×10^6 T cells in 100 μl PBS by tail-vein injection. Concurrent with adoptive cell transfer, mice were given a mixture of 20 μg of TLR9 ODN 2395 and 20 μg of ODN M363 (InvivoGen, San Diego, CA) for three days. To label T cells, CFSE (eBioscience, San Diego, CA) was diluted in dimethyl sulfoxide to yield a 5 mM stock solution. T cells were re-suspended to 5×10^7 cells/ml. A total of 1 μl of 0.5 mM CSFE was added to each ml of cells and incubated at 37 °C for 10 min. Cells were then washed twice with DMEM and twice with PBS before re-suspending in PBS at 1×10^7 cells/ml. We performed *retro*-orbital bleeds on a weekly basis throughout the study to monitor transaminase and bilirubin levels. We submitted the samples to Antech Diagnostics (Irvine, CA) for analysis.

2.4. Biodistribution

Liver samples were frozen on dry ice at the time of necropsy and DNA was extracted using the QIAamp DNA Mini Kit (Qiagen, Valencia, CA). We detected and quantified vector genome copies in the extracted DNA using real-time quantitative PCR (qPCR), as described previously [25]. Briefly, genomic DNA was isolated, and vector genome copies were quantified using primers/probes designed against the TBG promoter sequence of the vector. We quantified genome copies from the liver on one liver sample per mouse.

2.5. RNA analysis

Liver samples were frozen in liquid nitrogen at the time of necropsy. We extracted the RNA using TRIzol (Life Technologies, Carlsbad, CA) according to the manufacturer's protocol. A total of 12 μg of RNA was then treated with DNase I (Roche, Basel, Switzerland) according to the manufacturer's protocol. We used an RNeasy Mini Kit (Qiagen, Hilden, Germany) to remove DNase prior to cDNA synthesis by reverse transcription using the Applied Biosystems High Capacity cDNA Reverse Transcriptase Kit (Life Technologies). Real-time PCR was then performed on cDNA with primers binding to the h*OTC*co transgene with the Power SYBR Master Mix for detection (Life Technologies).

2.6. CD8 staining on frozen sections

Frozen liver sections were fixed in acetone at −20 °C for 7 min, air dried, and then blocked in 1% donkey serum (Jackson Immunoresearch Laboratories, West Grove, PA) in PBS for 20 min. The sections were then incubated with 1:20 primary rat Ab against CD8 (clone 53–6.7, BD Biosciences San Jose, CA) diluted in blocking buffer for 45 min. After washing in PBS, sections were stained with secondary donkey Abs labeled with FITC (Jackson Immunoresearch Laboratories) for 30 min, washed in PBS, and mounted in Vectashield immunofluorescence stain containing DAPI (Vector Laboratories, Burlingame, CA).

2.7. Ki-67 stain on paraffin sections

Paraffin sections were de-paraffinized through an ethanol and xylene series, boiled in a microwave for 6 min in 10 mM citrate buffer (pH 6.0 for antigen retrieval), and treated sequentially with 2% H_2O_2 (Sigma-Aldrich, St. Louis, MO) for 15 min, avidin/biotin blocking reagents (Vector Laboratories, Burlingame, CA) for 15 min, and blocking buffer (1% donkey serum [Jackson Immunoresearch, West Grove, PA] in PBS with 0.2% Triton) for 10 min. Sections were then incubated for one hour with 1:500 primary rabbit serum against Ki67 (ab15580, Abcam, Cambridge, United Kingdom) and for 45 min with FITC-labeled secondary donkey Ab (Jackson Immunoresearch) diluted in blocking buffer. Sections were mounted using Vectashield mounting medium (Vector Laboratories) containing DAPI as a nuclear counterstain.

2.8. Histopathology

Formalin-fixed paraffin-embedded tissue samples were sectioned and stained for H&E according to standard protocols. We scored histological sections using the following criteria: a hepatocellular necrosis score of 3 indicates multifocal, large clusters with hepatocellular loss; 2 indicates single-cell to multifocal clusters; 1 indicates single-cell necrosis; and 0 indicates no observed necrosis. Oval-cell hyperplasia was scored as follows: 3 indicates bridging or dissecting hepatocytes with architectural distortion; 2 indicates bridging or dissecting hepatocytes; 1 indicates focal or multifocal (periportal); and 0 indicates none. Inflammation, as determined by mixed mononuclear cell infiltration was scored as follows: 3 indicates marked, bridging, or dissecting hepatocytes or multifocal to coalescing within parenchyma; 2 indicates moderate, extending into surrounding periportal hepatocytes or multifocally within parenchyma; 1 indicates mild, few aggregates within portal areas and rare foci within parenchyma; and 0 indicates none. Hepatocellular regeneration was scored as follows: 3 indicates extensive hepatocellular karyocytomegaly with an average of 1–2 mitotic figures per lobule; 2 indicates moderate hepatocellular karyocytomegaly with an average of 0–1 mitotic figures per lobule; 1 indicates rare to periportal hepatocellular karyocytomegaly with rare mitotic figures; and 0 indicates none.

2.9. Statistics

We statistically analyzed the levels of ALT, AST, genome copies, and mRNA using a one-way ANOVA with a Bonferroni test in order to compare each group to the vector-only (hOTC) control. For image analysis experiments, we analyzed five images per mouse (N = 4). We used a one-way ANOVA with a Bonferroni test to statistically compare treatments to their day-appropriate control. We used a *t* test to analyze CD8 and tetramer-positive cells that were identified by flow cytometry.

2.10. Study approval

All of our procedures were performed using protocols that were preapproved by the University of Pennsylvania's Institutional Animal Care and Use Committee.

3. Results

3.1. Inflammation is required for a cytotoxic T-cell response

Previously, we showed that the presence of a strong inflammatory signal induces *T*-cell targeting of a transgene product, resulting in the loss of transgene expression and destruction of transduced cells in liver [26,27]. Here, we probed the role of TLR9 signaling in the initiation of a cytotoxic *T*-lymphocyte (CTL) response following AAV8 vector-mediated gene delivery of a codon-optimized human ornithine transcarbamylase (hOTCco). First, we developed a model system to evaluate transgene-specific immune responses to systemic inflammation caused by TLR9. In C57BL/6 mice, hOTC alone did not provoke a CTL response, even when expressed using an adenoviral vector that is known to elicit a strong immune response following i.m. administration (Supplemental Fig. 1). This lack of *T*-cell response may be due to the high level of protein homology (92%) between human and mouse OTC. Therefore, we generated a CTL response against the transgene by cloning a well-characterized peptide from chicken ovalbumin ($Ova_{257–264}$ SIINFEKL) to the C-terminus of h*OTC*co. We then adoptively transferred $CD8^+$ T cells from OT-1 mice, which are transgenic for a SIINFEKL-specific receptor found on all T cells, into wild-type C57BL/6 mice, in combination with a CpG oligodeoxynucleotide (ODN) cocktail as a TLR9 agonist. This method allowed us to study TLR9-mediated immune responses against the tagged h*OTC*co transgene product.

We initially treated C57BL/6 mice with an i.v. injection of an AAV8 vector expressing h*OTC*co-SIINFEKL from a liver-specific thyroxine-binding globulin (TBG) promoter (Fig. 1A). Fourteen days after vector injection, on study day 0, we adoptively transferred 1×10^6 SIINF-EKL-specific T cells from OT-1 mice. Concurrent with adoptive transfer, and over the next three days, C57BL/6 mice received 40 μg of CpG ODN via i.p. injection. Following the CpG ODN treatment in mice with both transgene-specific OT-1 T cells and TLR9 inflammatory signals, the levels of alanine transaminase (ALT) and aspartate transaminase (AST) were significantly elevated ($P < 0.001$; Fig. 1, B and C), indicating hepatocyte lysis. The livers of mice treated with both OT-1 T cells and CpG ODN showed a tenfold reduction in vector genome copy number ($P < 0.05$; Fig. 1D) and h*OTC*co-SIINFEKL mRNA expression ($P < 0.01$; Fig. 1E), consistent with T cell-mediated killing of transduced hepatocytes.

Next, we evaluated the relationship between the dose of adoptively transferred T cells and meaningful immune targeting of transduced hepatocytes. Our aim was to simulate a frequency of transgene-specific T cells that was representative of an endogenous, protein-specific, naïve *T*-cell population [28,29]. As few as 3,000 adoptively transferred cells elevated liver function ($P < 0.05$; Fig. 2, A–C) and decreased vector genome copies ($P < 0.05$; Fig. 2D). We also observed a significant reduction in transgene mRNA expression when we adoptively transferred 300,000 cells ($P < 0.05$; Fig. 2E). In these experiments, a CTL response to the transgene product occurred only when both transgene-specific OT-1 T cells and TLR9 inflammatory signals were present, suggesting that inflammation is required to activate CTL.

3.2. CTL activation leads to hepatocyte loss

In order to directly evaluate T cell-mediated killing of transduced cells in liver, we treated mice with vector, T cells, and CpG ODN. We subsequently sacrificed the mice at 3, 7, and 14 days after adoptive transfer to histologically evaluate the liver. We stained liver sections for $CD8^+$ T cells (Fig. 3A), and quantified infiltration by image analysis (Fig. 3B). Marked $CD8^+$ *T*-cell infiltration occurred at periportal and pericentral locations beginning on day 3 for mice that received OT-1 T cells regardless of TLR9 treatment. By day 7, infiltrates in mice treated with both T cells and CpG ODN penetrated deeper into the liver with infiltration resolving by day 14. By contrast, we did not observe further infiltration in mice that received T cells without TLR9 stimulation. In addition, we observed a loss of liver vector genome copies in mice treated with both T cells and CpG ODN; the greatest loss occurred between day 3 and day 14 post adoptive transfer (Supplemental Fig. 3A). These findings suggest that the elevation of transaminases by *T*-cell infiltration is due to T cell-mediated lysis of hepatocytes. Surprisingly, we did not observe significant differences between control and experimental groups in apoptosis, as detected by TUNEL staining (Supplemental Fig. 2A). This negative result could be due to the sampled time points, which may have missed the cell death of hepatocytes. Using Ki-67 staining to mark proliferation, we next measured the regeneration of hepatocytes that we predicted had undergone lysis based on transaminase elevation and vector genome loss. Hepatocyte division was spread evenly across liver regions in the experimental groups (Fig. 3C), mirroring the degree of $CD8^+$ *T*-cell infiltration. Hepatocyte division, defined as the percentage of hepatocytes that were Ki-67 positive, was significantly higher in the group that received both OT-1 transgenic $CD8^+$ T cells and CpG ODN than the expected turnover as represented by vector-treated controls ($P < 0.001$; Fig. 3D; [30,31]). To determine the extent of pathology associated with *T*-cell infiltration, we stained liver sections with H&E (Fig. 4E). We scored sections from 0 to 3 with severity increasing with score for monocyte infiltration (Fig. 4A), hepatocellular necrosis (Fig. 4B), hepatocellular regeneration (Fig. 4C), and oval-cell hyperplasia (Fig. 4D). On the seventh day, across all four measures, mice that received both ODN and OT-1 T cells had extensive histopathology, including the presence of multifocal clusters with extensive hepatocyte death and mixed mononuclear cell infiltration (lymphocytes, histocytes, and neutrophils). In these mice, we also observed extensive oval-cell hyperplasia with bridging to dissecting hepatocytes and architectural distortions. We also observed hepatocyte regeneration denoted by extensive hepatocellular karyocytomegaly with an average of one to two mitotic figures per lobule. By day 14, mice that had received the same treatment had negligible pathology in all four measures compared to untreated mice, indicating that the liver was resilient to the trauma of a T cell-mediated transgene-specific immune response. Together, these data indicate that the majority of *T*-cell infiltration and hepatocyte death occurs within a week after adoptive transfer and TLR9 stimulation.

3.3. TLR9 signaling results in T-cell expansion

We next examined whether the infiltrating cells were indeed transgene-specific CTLs. We labeled OT-1 transgenic $CD8^+$ T cells with carboxyfluorescein succinimidyl ester (CFSE) fluorescent dye before delivering the cells into C57BL/6 mice that were previously treated with h*OTC*co-SIINFEKL. Seven days after adoptive transfer and TLR9 stimulation, we isolated lymphocytes from the spleen and liver and stained them with anti-CD8α and

SIINFEKL tetramer (Fig. 5, A–D). Only a minority of spleen-isolated $CD8^+$ T cells were tetramer positive (Fig. 5, A and B), although mice that received CpG ODN had a significantly higher proportion of tetramer-positive cells ($P < 0.01$). In contrast, the majority of liver-isolated $CD8^+$ lymphocytes were tetramer positive, regardless of whether mice received CpG ODN. This result indicates that even without inflammation, additional inflammatory signals from an acute event modeled by ODN administration of transgene-specific T cells can migrate to the liver if the transgene is present in hepatocytes (Fig. 5, C and D). In addition, CFSE staining of tetramer-positive liver-isolated T cells remained high in mice that did not receive CpG ODN, whereas CFSE staining was diluted in mice treated with CpG ODN (Fig. 5, E and F). This finding suggests that in the presence of TLR9 stimulation, transgene-specific $CD8^+$ T cells undergo increased proliferation, which is marked by the dilution of CFSE. This finding contrasts with our observations in mice that did not receive ODN administration.

3.4. Intrinsic TLR9 signaling in T cells is insufficient to activate an immune response

As systemic administration of CpG ODN-induced *T*-cell activation against the transgene product, we next explored whether autocrine signaling by TLR9 in donor T cells would be sufficient to trigger an immune response or whether paracrine signaling, potentially from TLR9-expressing recipient plasmacytoid dendritic cells [32], is required for this effect. We injected C57BL/6 or TLR9 −/− mice i.v. with h*OTC*co-SIINFEKL. Fourteen days later, we adoptively transferred 1×10^6 OT-1 $CD8^+$ T cells into recipient mice that were also given CpG ODN as before (see schematic in Fig. 6A). Transaminase elevation occurred only in the C57BL/6 group, indicating that intact TLR9 signaling in transferred OT-1 T cells was insufficient to activate a robust CTL response (Fig. 6, B and C). Consistent with these results, both genome copy and transgene mRNA loss were profound in C57BL/6 but not TLR9 −/− mice (Fig. 6, D and E). Therefore, the TLR9 signaling that is required for initiating *T*-cell responses must be extrinsic to the T cells themselves, and perhaps occurs in transduced hepatocytes or antigen-presenting cells.

4. Discussion

Adaptive immune responses to a transgene product are complex and researchers consider many factors when optimizing vector delivery, including route of administration, vector design, residual target gene expression, and diseased state of the target organ. These factors can dramatically affect the likelihood that a given therapy will induce an inflammatory environment, elicit an adaptive anti-transgene response, and lead to an ineffective treatment [6,19,33]. Here, we show that loss of TLR9 signaling, or high affinity transgene specific T cells dramatically attenuates CTL immune responses against the transgene following i.v. administration of an AAV vector.

TLR9 activation induced a robust *T*-cell response against the transgene product resulting in a loss of vector genomes that accompanied cellular infiltration and tissue necrosis. The hepatitis was selflimiting and the inflammation resolved by day 14 accompanied by cellular division. Interestingly, we did not observe any apoptosis in the liver sections, as evaluated by TUNEL staining. We did, however, note the loss of AAV genomes, histopathological

evidence of necrosis in H&E sections, and highly elevated liver enzymes. We suggest two possible mechanisms for this observed discrepancy. The first possibility, based on our data, is that cell division accompanies hepatocyte cell death by necrosis as the liver recovers from the insult. Cell division contributes to a reduction in liver genome copies due to the dilution of vector genomes. Alternatively, it is possible that cell division is primarily responsible for the loss of genome copies, which are not retained when the nuclear envelope is dissolved and reformed. Proliferation in the absence of hepatocyte death could be a consequence of immune activation by TRL9 signaling. Indeed, many of the innate immune cells that migrated to the region of *T*-cell infiltration, including macrophages and dendritic cells, are involved in an IL6-mediated pathway that activates hepatocyte proliferation [34,35]. This would be a complicating outcome for AAV-based gene therapy if a loss of treatment efficacy by dilution of vector genomes could occur without transgene-specific *T*-cell activation, but merely by a transient innate immune response. However, the results of our first experiment indicate that while there is a trend toward expression loss in the ODN-only treated group (inflammation), this result was not significant. By contrast, our data, which showed that *T*-cell activation was required for expression loss, was consistent across multiple experiments and the genome copy loss was significant. Thus the immunological response that is necessary to lose the efficacy of AAV gene therapy must be more than an innate immune response. We suggest that researchers should avoid both of these outcomes and explore strategies to reduce inflammation [36].

Liver targeted AAV gene therapy clinical trials have thus far had minimal findings of *T*-cell responses to the transgene product. One exception to this was an early hemophilia clinical trial where acute liver toxicity in conjunction with the presence of AAV2 capsid-specific T cells in peripheral blood mononucleocytes (PBMCs) was considered a potential cause of attenuated transgene expression [37]. This finding was also shown in the high dose cohorts of another AAV hemophilia trail, this time with AAV8, though use of steroids at early signs of liver toxicity minimized expression loss [1]. These findings for capsid-specific T cells and the general lack of evidence for transgene-specific T cells from human clinical trials could be used to argue that transgene-specific immune responses are an unlikely outcome of liver targeted gene therapy. However, some of our work in non-human primate studies has shown that despite a lack of transgene-specific T cells in PBMCs, resident liver T cells were activated against the transgene, UGT1A1, though the minimal liver toxicity did not impact transgene expression [38]. Together these results suggest that is possible for individuals to have transgene-specific resident liver T cells that would be missed by analysis of PBMCs, and similarly not induce a transgene attenuating immune response. Our work here suggests that to induce a transgene attenuating immune response the stimuli would need to be more impactful than that of the AAV delivery alone, perhaps in conjunction with the underlying disease state of the liver. Likewise cytotoxic T cells would need to have HLA with high affinity for transgene epitopes, an event thought to occur more often in individuals lacking cross reactive material [39]. Under these conditions we could anticipate observing a liver toxic transgene specific immune response.

4.1. Conclusions

When considering the implications of these results for clinical trials of AAV gene therapy, researchers should focus on the underlying sources of inflammation. Inflammatory stimulus could occur as a result of the route of administration, or the underlying pathology of the target organ. The HLA haplotype could also exacerbate vector-directed adaptive immunity. However, our studies demonstrate that TLR9 recognition of AAV vector genomes is a primary source of inflammation and scientists should consider strategies to reduce TLR9 activation. We previously demonstrated that CpG di-nucleotides in the vector genome elicit transgene-specific adaptive immune responses in the context of a pro-inflammatory capsid, and that removing such CpG motifs could eliminate transgene clearance [21]. We expect these results to help guide the conversation when considering the impact of transgene-specific *T*-cell toxicity on AAV-mediated gene transfer.

Supplementary Material

Refer to Web version on PubMed Central for supplementary material.

Acknowledgements

We acknowledge the support of the Penn Vector Core, Christine Draper, and Deirdre McMenamin of the Program for Comparative Medicine. We thank Elizabeth L. Buza for histopathological analyses. We thank Hongwei Yu and Yanqing Zhu for invaluable technical assistance.

Funding sources

This work was supported by the National Institute of Child Health and Human Development [P01HD057247].

Abbreviations:

TLR9	Toll-like receptor 9
OTC	ornithine transcarbamylase
AAV	adeno-associated virus
ODN	Oligodeoxynucleotide
CSFE	Carboxyfluorescein succinimidyl ester
AST	Aspartate transaminase
ALT	Alanine transaminase
CLT	Cytotoxic *T*-lymphocyte
TBG	Thyroxine-binding globulin
PBMC	peripheral blood mononucleocytes

References

[1]. Nathwani AC, Reiss UM, Tuddenham EG, et al., Long-term safety and efficacy of factor IX gene therapy in hemophilia B, The New England J. Med 371 (21) (2014) 1994–2004. [PubMed: 25409372]

[2]. Jacobson SG, Cideciyan AV, Roman AJ, et al., Improvement and decline in vision with gene therapy in childhood blindness, N. Engl. J. Med 372 (20) (2015) 1920–1926. [PubMed: 25936984]

[3]. Simonelli F, Maguire AM, Testa F, et al., Gene therapy for Leber's congenital amaurosis is safe and effective through 1.5 years after vector administration, Mol. Ther 18 (3) (2010) 643–650. [PubMed: 19953081]

[4]. Gene Naldini L., therapy returns to centre stage, Nature 526 (7573) (2015) 351–360 10/15/print. [PubMed: 26469046]

[5]. Nayak S, Doerfler PA, Porvasnik SL, et al., Immune responses and hypercoagulation in ERT for Pompe disease are mutation and rhGAA dose dependent, PLoS One 9 (6) (2014) e98336. [PubMed: 24897114]

[6]. Cao O, Hoffman BE, Moghimi B, et al., Impact of the underlying mutation and the route of vector administration on immune responses to factor IX in gene therapy for hemophilia B, Mol. Ther 17 (10) (2009) 1733–1742. [PubMed: 19603001]

[7]. Finn JD, Ozelo MC, Sabatino DE, et al., Eradication of neutralizing antibodies to factor VIII in canine hemophilia A after liver gene therapy, Blood 116 (26) (2010) 5842–5848. [PubMed: 20876851]

[8]. Hinderer C, Bell P, Louboutin JP, et al., Neonatal Systemic AAV Induces Tolerance to CNS Gene Therapy in MPS I Dogs and Nonhuman Primates, Mol. Ther 23 (8) (2015) 1298–1307. [PubMed: 26022732]

[9]. Ding EY, Hodges BL, Hu H, et al., Long-term efficacy after [E1-, polymerase-] adenovirus-mediated transfer of human acid-alpha-glucosidase gene into glycogen storage disease type II knockout mice, Hum. Gene Ther 12 (8) (2001) 955–965. [PubMed: 11387060]

[10]. Fields PA, Kowalczyk DW, Arruda VR, et al., Role of Vector in Activation of T Cell Subsets in Immune Responses against the Secreted Transgene Product Factor IX, Mol. Ther 1 (3) (2000) 225–235 03//print. [PubMed: 10933938]

[11]. Limberis MP, Figueredo J, Calcedo R, Wilson JM, Activation of CFTR-specific T Cells in cystic fibrosis mice following gene transfer, Mol. Ther 15 (9) (2007) 1694–1700. [PubMed: 17579582]

[12]. Ciesielska A, Hadaczek P, Mittermeyer G, et al., Cerebral infusion of AAV9 vector-encoding non-self proteins can elicit cell-mediated immune responses, Mol. Ther 21 (1) (2013) 158–166. [PubMed: 22929660]

[13]. Bradbury AM, Cochran JN, McCurdy VJ, et al., Therapeutic response in feline sandhoff disease despite immunity to intracranial gene therapy, Mol. Ther 21 (7) (2013) 1306–1315. [PubMed: 23689599]

[14]. Lang KS, Georgiev P, Recher M, et al., Immunoprivileged status of the liver is controlled by Toll-like receptor 3 signaling, J. Clin. Investig 116 (9) (2006) 2456–2463. [PubMed: 16955143]

[15]. Rogers GL, Martino AT, Aslanidi GV, Jayandharan GR, Srivastava A, Herzog RW, Innate Immune Responses to AAV Vectors, Front. Microbiol 2 (2011) 194. [PubMed: 21954398]

[16]. Hemmi H, Takeuchi O, Kawai T, et al., A Toll-like receptor recognizes bacterial DNA, Nature 408 (6813) (2000) 740–745. [PubMed: 11130078]

[17]. Zhu J, Huang X, Yang Y, The TLR9-MyD88 pathway is critical for adaptive immune responses to adeno-associated virus gene therapy vectors in mice, J. Clin. Investig 119 (8) (2009) 2388–2398. [PubMed: 19587448]

[18]. Zaiss AK, Liu Q, Bowen GP, Wong NC, Bartlett JS, Muruve DA, Differential activation of innate immune responses by adenovirus and adeno-associated virus vectors, J. Virol 76 (9) (2002) 4580–4590. [PubMed: 11932423]

[19]. Martino AT, Suzuki M, Markusic DM, et al., The genome of self-complementary adeno-associated viral vectors increases Toll-like receptor 9-dependent innate immune responses in the liver, Blood 117 (24) (2011) 6459–6468. [PubMed: 21474674]

[20]. Reyes-Sandoval A, Ertl HC, CpG methylation of a plasmid vector results in extended transgene product expression by circumventing induction of immune responses, Mol. Ther 9 (2) (2004) 249–261. [PubMed: 14759809]

[21]. Faust SM, Bell P, Cutler BJ, et al., CpG-depleted adeno-associated virus vectors evade immune detection, J. Clin. Investig 123 (7) (2013) 2994–3001. [PubMed: 23778142]

[22]. Shapir N, Miari R, Blum S, et al., Preclinical and preliminary clinical evaluation of genetically transduced dermal tissue implants for the sustained secretion of erythropoietin and interferon alpha, Hum. Gene Ther. Clin. Dev (2015).

[23]. Haas T, Metzger J, Schmitz F, et al., The DNA sugar backbone 2' deoxyribose determines toll-like receptor 9 activation, Immunity 28 (3) (2008) 315–323. [PubMed: 18342006]

[24]. Lock M, Alvira M, Vandenberghe LH, et al., Rapid, simple, and versatile manufacturing of recombinant adeno-associated viral vectors at scale, Hum. Gene Ther 21 (10) (2010) 1259–1271. [PubMed: 20497038]

[25]. Bell P, Moscioni AD, McCarter RJ, et al., Analysis of Tumors Arising in Male B6C3F1 Mice with and without AAV Vector Delivery to Liver, Mol. Ther 14 (1) (2006) 34–44 07//print. [PubMed: 16682254]

[26]. Breous E, Somanathan S, Bell P, Wilson JM, Inflammation promotes the loss of adeno-associated virus-mediated transgene expression in mouse liver, Gastroenterology 141 (1) (2011) 348–57, 57.e1–3. [PubMed: 21640112]

[27]. Somanathan S, Breous E, Bell P, Wilson JM, AAV vectors avoid inflammatory signals necessary to render transduced hepatocyte targets for destructive T cells, Mol. Ther 18 (5) (2010 5) 977–982. [PubMed: 20234342]

[28]. Jenkins MK, Moon JJ, The role of naive T cell precursor frequency and recruitment in dictating immune response magnitude, J. Immunol. (Baltimore, Md : 1950) 188 (9) (2012) 4135–4140.

[29]. Moon JJ, Chu HH, Pepper M, et al., Naive CD4(+) T cell frequency varies for different epitopes and predicts repertoire diversity and response magnitude, Immunity 27 (2) (2007) 203–213. [PubMed: 17707129]

[30]. Miyaoka Y, Ebato K, Kato H, Arakawa S, Shimizu S, Miyajima A, Hypertrophy and unconventional cell division of hepatocytes underlie liver regeneration, Curr Biol 22 (2012).

[31]. Miyaoka Y, Miyajima A, To divide or not to divide: revisiting liver regeneration, Cell Division 8 (1) (2013) 1–12. [PubMed: 23286511]

[32]. Rogers GL, Shirley JL, Zolotukhin I, et al., Plasmacytoid and conventional dendritic cells cooperate in crosspriming AAV capsid-specific CD8(+) T cells, Blood 129 (24) (2017) 3184–3195. [PubMed: 28468798]

[33]. Rogers GL, Martino AT, Zolotukhin I, Ertl HC, Herzog RW, Role of the vector genome and underlying factor IX mutation in immune responses to AAV gene therapy for hemophilia B, J. Transl. Med 12 (2014) 25. [PubMed: 24460861]

[34]. Aldeguer X, Debonera F, Shaked A, et al., Interleukin-6 from intrahepatic cells of bone marrow origin is required for normal murine liver regeneration, Hepatology (Baltimore, MD) 35 (1) (2002) 40–48.

[35]. Cressman DE, Greenbaum LE, DeAngelis RA, et al., Liver failure and defective hepatocyte regeneration in interleukin-6-deficient mice, Science (New York, NY). 274 (5291) (1996) 1379–1383.

[36]. Greig JA, Nordin JML, White JW, et al., Optimized adeno-associated viral-mediated human factor VIII gene therapy in cynomolgus macaques, Hum. Gene Ther (2018).

[37]. Manno CS, Pierce GF, Arruda VR, et al., Successful transduction of liver in hemophilia by AAV-Factor IX and limitations imposed by the host immune response, Nat Med. 12 (3) (2006 3) 342–347. [PubMed: 16474400]

[38]. Greig JA, Calcedo R, Kuri-Cervantes L, et al., AAV8 Gene Therapy for Crigler-Najjar Syndrome in Macaques Elicited Transgene T Cell Responses That Are Resident to the Liver, Mol Ther Methods Clin Dev. 14 (11) (2018) 191–201.

[39]. Kishnani PS, Goldenberg PC, DeArmey SL, et al., Cross-reactive immunologic material status affects treatment outcomes in Pompe disease infants, Mol Genet Metab. 99 (1) (2010) 26–33. [PubMed: 19775921]

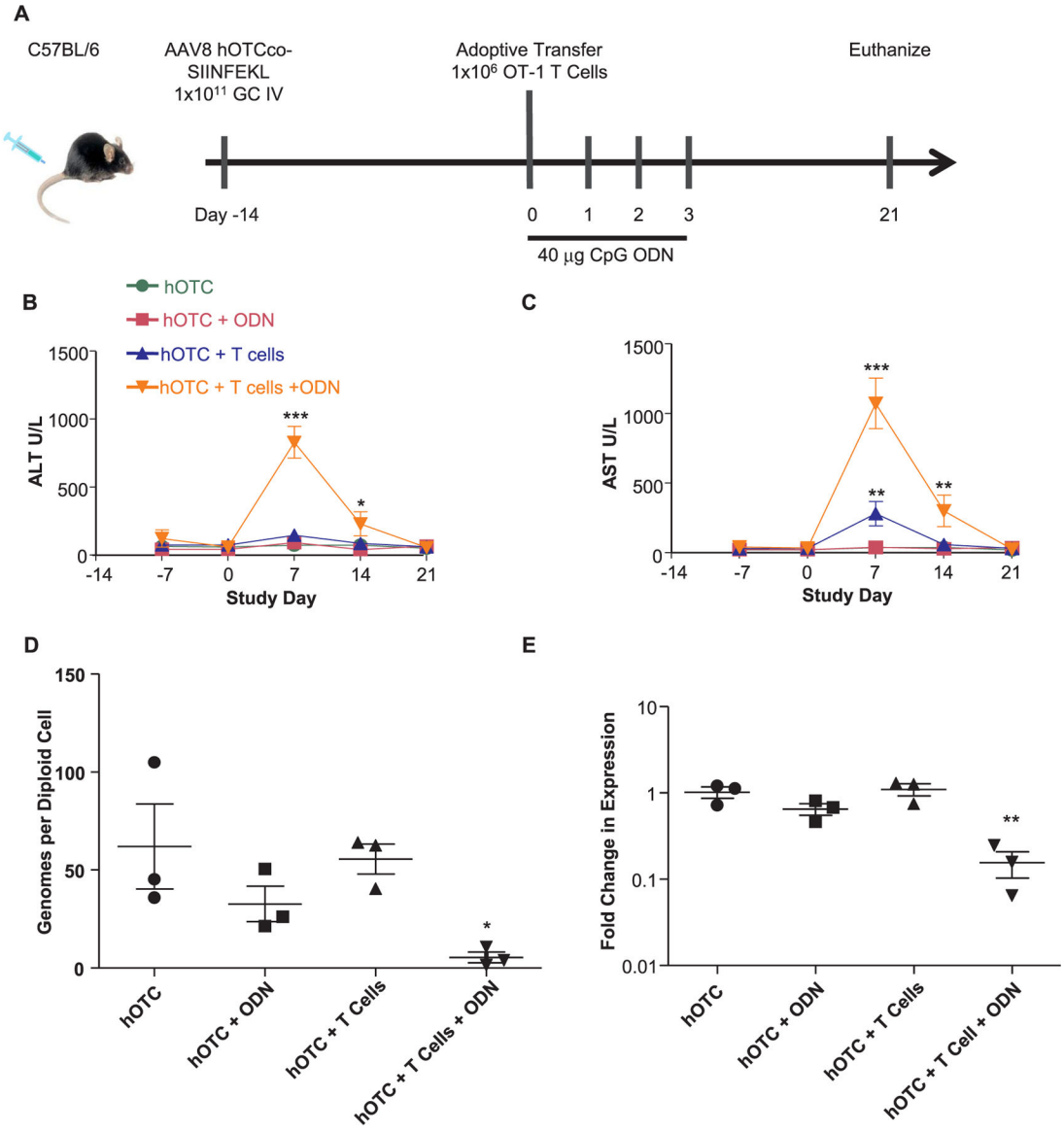

Fig. 1.

Systemic inflammation breaks tolerance to a transgene product. (A) A schematic of the experimental design detailing i.v. administration of AAV8 expressing hOTCco-SIINFEKL 40 µg CpG ODN for three days following adoptive transfer. Serum (B) ALT and (C) AST levels were monitored every seven days following vector delivery. (D) Genome copy and (E) transgene mRNA levels from liver were determined using qPCR after the study terminated. These experiments were independently performed three times; here we show representative results (N = 3). Statistical analysis by ANOVA with a Bonferroni posttest to vector only control. $*P < 0.05$, $**P < 0.001$, $***P < 0.0001$. Error Bars = SEM.

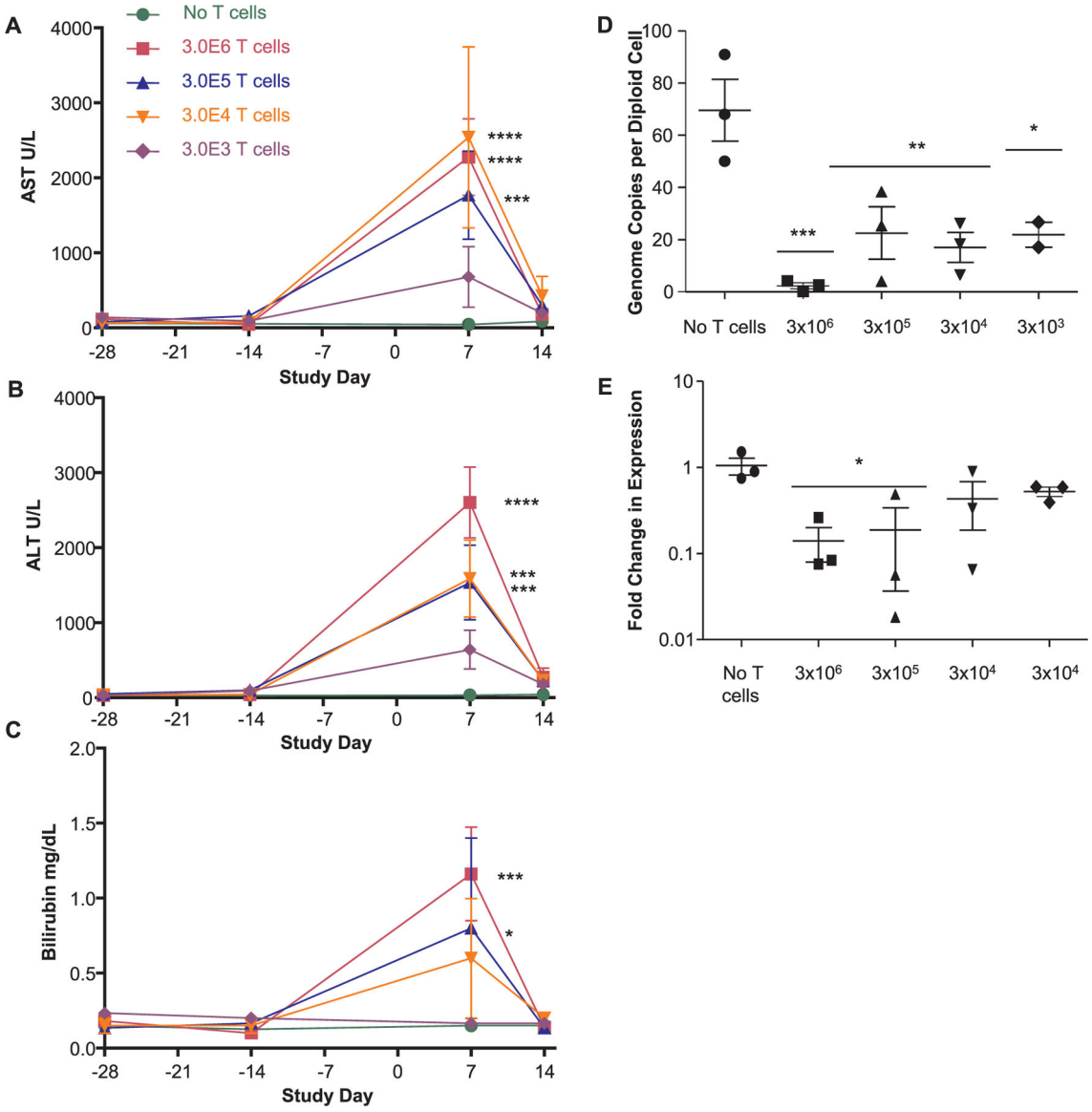

Fig. 2.

Effect of *T*-cell population on immune response. Mice received i.v. injections of AAV8 expressing hOTCco-SIINFEKL; 28 days after vector delivery, we transferred OT-1 $CD8^+$ T cells to recipient mice concurrent with an administration of 40 μg of CpG ODN. Serum (A) AST, (B) ALT, and (C) bilirubin levels were monitored every seven days following vector delivery. (D) Genome copy and (E) transgene mRNA levels from liver were determined by qPCR following the termination of the study. N = 3. Statistical analysis by ANOVA with a Bonferroni posttest to vector only control. *$P < 0.05$, **$P < 0.001$, ***$P < 0.0001$, ****$P < 0.00001$. Error Bars = SEM.

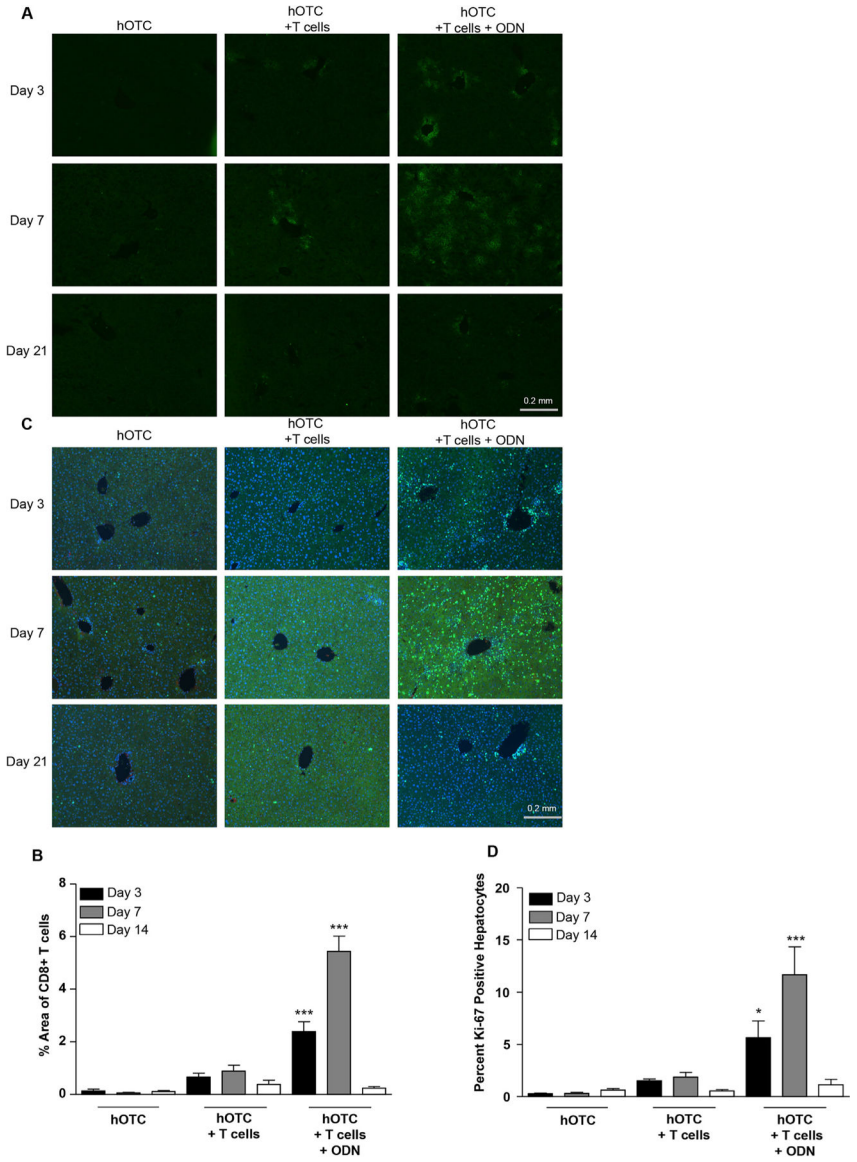

Fig. 3.

T-cell infiltration and hepatocyte proliferation. Mice received i.v. injections of the vector and, 14 days later, OT-1 $CD8^+$ T cells were transferred concurrent with an administration of 40 μg CpG ODN. Mice were sacrificed on days three, seven, and 14 following adoptive transfer. (A) We stained liver sections for CD8, and (B) we determined the percent area covered by infiltrating T cells using Image J. (C) We stained liver sections with the Ki-67 proliferation marker, and (D) calculated percent positive hepatocytes. For image analysis experiments, we analyzed five images per mouse. N = 4 Statistical analysis by ANOVA with a Bonferroni posttest to day appropriate vector only control. . $*P < 0.05$, $***P < 0.0001$. Error Bars = SEM.

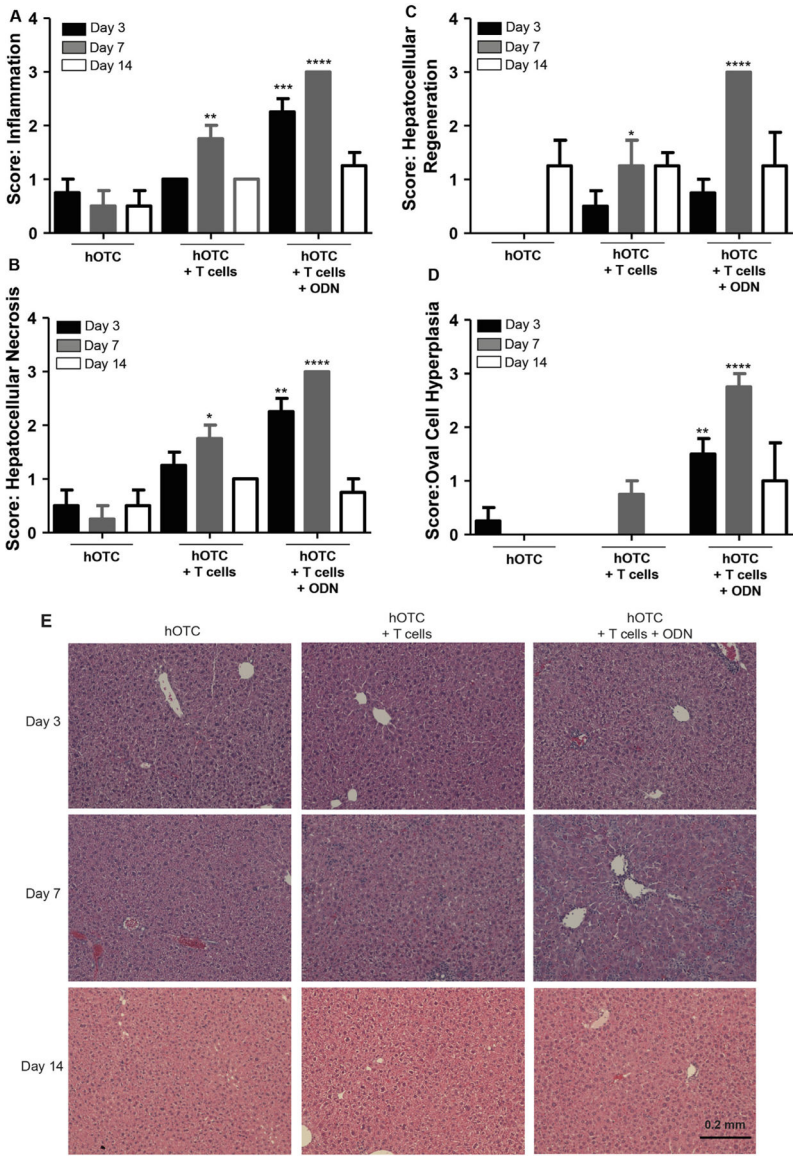

Fig. 4.

Liver pathology following adoptive transfer. Mice received i.v. injections of the vector and, 14 days later, OT-1 $CD8^+$ T cells were transferred concurrent with an administration of 40 μg CpG ODN. Mice were sacrificed on days three, seven, and 14 following adoptive transfer. We stained liver sections for H&E and scored for extent of (A) inflammation, (B) hepatocellular necrosis, (C) hepatocellular regeneration, and (D) oval-cell hyperplasia. (E) The histopathologic images depicted represent general trends for each dose group. Statistical analysis by student *t* test. $*P < 0.05$, $**P < 0.001$, $***P < 0.0001$. $****P < 0.00001$. Error Bars = SEM.

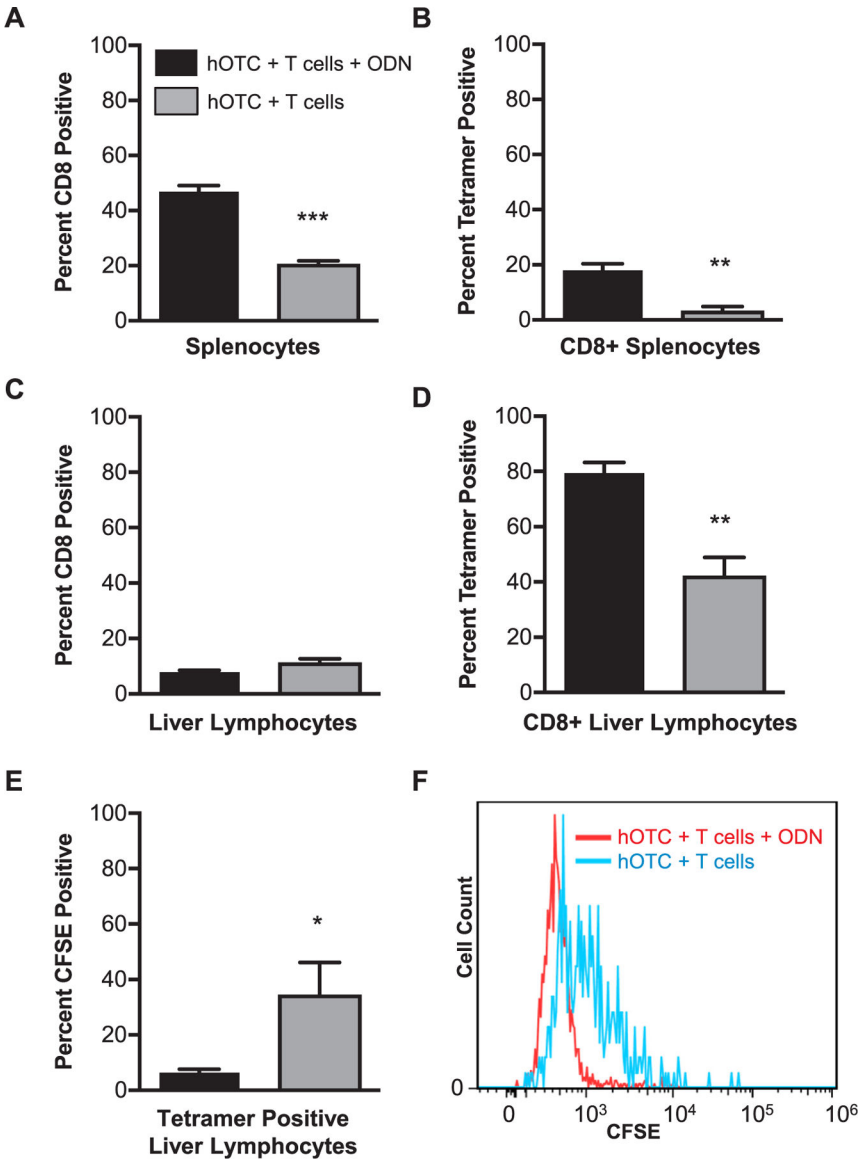

Fig. 5.

Transgene-specific *T*-cell infiltration. Mice were given AAV8 hOTCco-SIINFEKL; 14 days later, we administered the CpG ODN and CFSE-labeled OT-1 $CD8^+$ T cells. Mice were sacrificed seven days following $CD8^+$ *T*-cell transfer, and we isolated lymphocytes from the liver and spleen. Lymphocytes isolated from the (A) spleen and (C) liver by forward and side scatter were stained for CD8. (B) Spleen-and (D) liver-isolated $CD8^+$ T cells were stained with SIINFEKL tetramer. (E) We analyzed tetramer-positive liver lymphocytes for CFSE retention. (F) Here we show a representative single parameter histogram for analysis of CFSE retention in cell populations with and without CpG ODN treatment. N = 4. $*P < 0.05$, $**P < 0.001$. Error Bars = SEM.

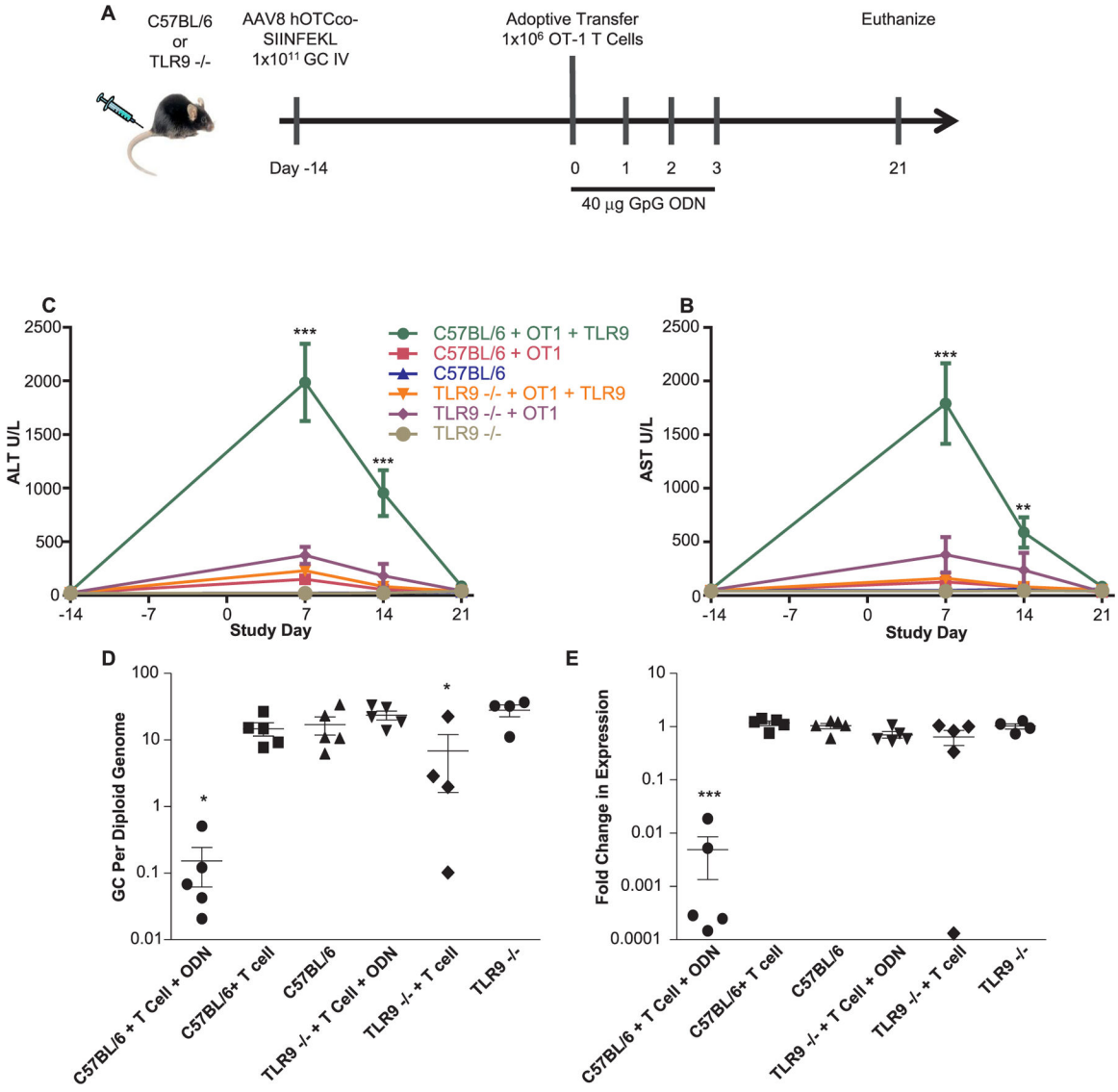

Fig. 6.

Extrinsic TLR9 signaling is required for a destructive CTL response. (A) A schematic of the study design. C57BL/6 or TLR9 −/− mice received i.v. injections of AAV8 expressing hOTCco-SIINFEKL. Fourteen days after vector delivery, OT-1 $CD8^+$ T cells were transferred to recipient mice concurrent with an administration of 40 µg of CpG ODN, which was also administered for three days following adoptive transfer. We monitored serum (B) AST and (C) ALT levels every seven days following vector delivery. Following the termination of the study, we determined the levels of (D) genome copy and (E) transgene mRNA expression levels. N = 5. Statistical analysis by ANOVA with a Bonferroni posttest to vector only control. $*P < 0.05$, $**P < 0.001$, $***P < 0.0001$. Error Bars = SEM.